



# Architecture of the subcontinental lithospheric mantle of the Archean segment of the Fennoscandian Shield: Analysis of seismic data

A.A. Meshcheryakova<sup>a,\*</sup>, A.I. Slabunov<sup>a</sup>, N.V. Vaganova<sup>b</sup>, M.D. Rychanchik<sup>a</sup>

<sup>a</sup> Institute of Geology of the Karelian Research Centre of the Russian Academy of Sciences, 11 Pushkinskaya Str., Petrozavodsk 185914, Russia

<sup>b</sup> N. Laverov Federal Center for Integrated Arctic Research of the Ural Branch of the Russian Academy of Sciences, 23, Severnoj Dviny Emb., Arkhangelsk 163000, Russia

## ARTICLE INFO

### Keywords:

Subcontinental lithospheric mantle  
Velocity model  
Archean  
Fennoscandian Shield  
Seismic data  
Receiver functions method

## ABSTRACT

Here, Karelian seismological network data were studied to reveal the architecture of the subcontinental lithospheric mantle (SCLM). The receiver functions method was used, which is based on the identification of converted waves from teleseismic earthquakes and their joint inversion into a velocity model. Original one-dimensional (1D) velocity models for the continental lithosphere of the central Karelian Craton (KC) and the western Belomorian Mobile Belt (BMB; both part of the Archean segment of the Fennoscandian Shield) were presented, analysed and interpreted in geological and petrological terms.

The obtained results reveal that the SCLM is >200 km thick both in the KC and the BMB. The mantle in both structures was shown to contain a well-defined, contrasting boundary with the crust. However, the boundary between the SCLM and the asthenosphere was not identified in this study. The SCLM was found to be stratified and divided into upper, middle and lower layers in both structures. The boundary between the upper and middle layers was identified at a depth near the upper line of the garnet stability limit in mantle peridotites; the boundary between the middle and lower layers corresponds to the graphite/diamond equilibrium line.

The SCLM of the BMB was shown to exhibit a distinct lowered velocity zone in the middle layer. The 1D velocity model of the central KC was found to be in good agreement with the evidence for the SCLM stratigraphy, based on the study of mantle xenoliths and xenocrysts from kimberlites and lamproites from the area.

## 1. Introduction

A subcontinental lithospheric mantle (SCLM) – it is part of the lithosphere under the crust. Being the main part of the lithosphere, the thickness, composition, and architecture of the SCLM consistently vary with time and are interrelated with crustal evolution (Griffin et al., 2003). Studying the SCLM of Archean cratons is essential for better understanding the Earth's early evolution, which is one of the crucial and fundamental tasks in geosciences (Khain, 2003; NASEM (National Academies of Sciences, Engineering, and Medicine), 2020; Windley et al., 2021).

Archean continental lithospheres have thicknesses of >200 km (Artemieva and Mooney, 2001). Archean lithospheric areas with thicknesses >200 km are called lithospheric keels, and their diverse compositions are controlled by several evolutionary factors (Artemieva, 2011; Griffin and O'Reilly, 2019). Old lithosphere has typically been affected by active geodynamic processes such as mantle plumes or subduction activities and may have undergone significant restructuring,

with examples including the North China and Indian shields (Xu, 2001; Shaikh et al., 2020). In these cases, the composition and structure of the mantle were altered, along with the characteristics of their geophysical fields. The Archean lithosphere of the eastern Fennoscandian Shield is one of the thickest and likely best preserved lithospheric areas worldwide (Artemieva, 2011), despite the multiple effects of active geodynamic processes that have influenced it following the Archean. The shield consists of an old core (Fig. 1) comprising the Archean Karelian Craton (KC) and the Archean-Proterozoic Belomorian Mobile Belt (BMB) (Slabunov et al., 2006a, b). In both provinces, the SCLM and crust were primarily formed during the Archean; however, the BMB was altered as part of an orogeny that occurred during the Paleoproterozoic. Both provinces were repeatedly (in both the Proterozoic and the Paleozoic) affected by mantle plumes (Kulikov et al., 2017).

The thickness and architecture of the lithosphere in the study area have been previously studied using seismic tomography (for example SVEKALAPKO, POLENET/LAPNET) (Sandoval et al., 2004; Hjelt et al., 2006; Tsvetkova et al., 2010, 2019; Sharov, 2004; Silvenoinen et al.,

\* Corresponding author.

E-mail addresses: [ademeshch@gmail.com](mailto:ademeshch@gmail.com) (A.A. Meshcheryakova), [slabunov@krc.karelia.ru](mailto:slabunov@krc.karelia.ru) (A.I. Slabunov).

<https://doi.org/10.1016/j.tecto.2022.229541>

Received 21 December 2021; Received in revised form 20 July 2022; Accepted 6 August 2022

Available online 19 August 2022

0040-1951/© 2022 Elsevier B.V. All rights reserved.

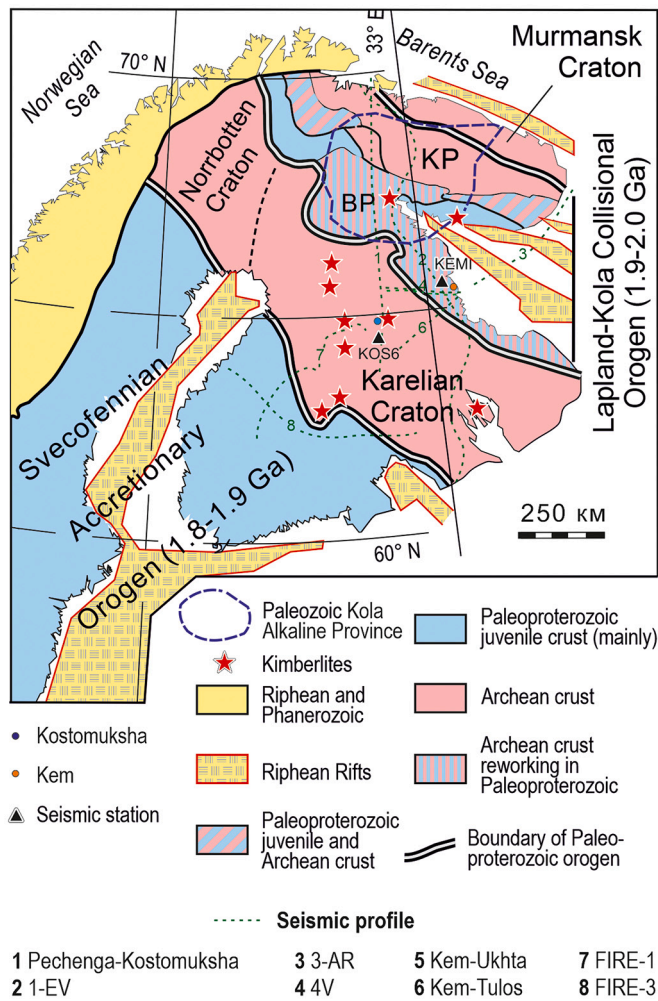


**Fig. 1.** Tectonic division of the Fennoscandian Shield (Baluev et al., 2012; Slabunov, 2008; Balagansky et al., 2015; O’Brain et al., 2005), distribution of seismic profiles and locations of KOS6 and KEMI seismic stations.

2016), seismic geo-traverse data (Sharov, 2017), thermometry (Kukkonen and Peltonen, 1999; Artemieva, 2006, 2009; Artemieva et al., 2006), and mantle xenoliths and xenocrysts in kimberlite-lamproite (Peltonen et al., 2002; Lehtonen et al., 2004; O’Brain et al., 2005; Peltonen and Brüggmann, 2006; Lehtonen and O’Brien, 2009; Zozulya et al., 2009).

In total these data determine the stratification and thickness of the lithosphere within the Archean segment of 220–275 km.

The lithosphere of the craton was studied in its western part, and data from the Karelian Seismological Network supplement the knowledge about the eastern part of the structure.

Karelian Seismological Network stations KOS6 and KEMI (See Table 1), which have both been functioning since 2004 (Sharov, 2004), are located within the KC and BMB, respectively. The network was updated in 2014 (Lebedev and Meshcheryakova, 2014) to record teleseismic earthquakes, and it uses the receiver function method to construct lithospheric velocity models (Vinnik, 1977, Vinnik, 1977,

**Table 1**  
Initial data.

s/s	Station coordinates	Number of events N	Mean distance, degrees	Mean azimuth, degrees	Depth, km	Magnitude
KOS6	Lat = 64.59	PRF 92	PRF 64.8	PRF 110.9	2–461	5.5–7.9
	Lon = 30.59	SRF 26	SRF 83.6	SRF 163.06		
KEMI	Lat = 65.04	PRF 97	PRF 69.6	PRF 117.9	5–686	5.2–7.9
	Lon = 33.67	SRF 33	SRF 83.1	SRF 168.6		

Farra and Vinnik, 2000) to a depth of up to 300 km. Previous researchers (Vinnik et al., 2007, Farra and Vinnik, 2000, Hjelt et al., 2006) studied the eastern side of the Paleoproterozoic Svecofennian belt and its border area with the Archean craton. Herein, new one-dimensional (1D) velocity models of the continental lithosphere for the central KC and western BMB were analysed to interpret available seismic data in terms of geology and petrology.

**2. Geology and deep structure of the Eastern Fennoscandian shield**

The eastern Fennoscandian Shield (Fig. 1) comprises the Archean Norrbotten, Karelian, and Murmansk cratons, as well as the Paleoproterozoic Lapland–Kola collisional orogen, which includes the Archean Kola Province and BMB (Daly et al., 2006; Slabunov et al., 2006a; Hölttä et al., 2014). The KC borders with the Paleoproterozoic Svecofennian accretionary orogen in the west (Lahtinen et al., 2008; Baltybaev, 2013) (Fig. 1).

A rift system was formed in the Fennoscandian Shield during the Meso-Neoproterozoic (Baluev, 2016; Baluev et al., 2012), accompanied by kimberlite magmatism (Bogatikov et al., 2007). In the Paleozoic (Devonian), the lithosphere was affected by the Kola mantle plume, resulting as the Kola alkaline province (Fig. 1) with alkaline, carbonate, and kimberlite magmatism (Arzamastsev et al., 2009). Thus, the continental lithosphere of the KC and BMB was formed during the Archean and then modified by various tectono-thermal alterations in the Proterozoic and Phanerozoic.

**2.1. Geology and deep lithospheric structure of the KC**

The KC comprises mildly metamorphosed granite–greenstone complexes of Archean (3.5–2.7 Ga) containing the relicts of granulites (Rybakov et al., 1981; Glebovitsky, 2005; Slabunov et al., 2006a; Hölttä et al., 2012). During the Proterozoic, rift basins, mafic layered intrusions, and a few generations of dikes, kimberlites, and lamproites were formed in the KC (Sokolov, 1987; O’Brain et al., 2005; Bogatikov et al., 2007; Glushanin et al., 2011; Gorkovets and Sharov, 2015; Kulikov et al., 2017).

The velocity seismic tomography (Sandoval et al., 2004; Hjelt et al., 2006; Tsvetkova et al., 2010, 2019; Sharov, 2004) for the central part of the craton has indicated that there are substantial lateral heterogeneities, based on Pechenga–Kostomuksha profile and SVEKALAPKO experiment data. The KC crust varies in thickness from 35 to 60 km (Sharov, 2017); it is 38 km thick near Seismic Station KOS6 (Mitrofanov et al., 1998). This implies that there is a local decline in velocity at depths of 40–80 km in the area of Kostomuksha, passing eastward into a region of locally increased velocity at the same depth range (Zolotov et al., 2000; Sharov, 2017). But among 1-D model (station JOF) for western KC there are two high-velocity layers (S-wave velocity + 4–6% relative to IASP91) from 40 to 80 km and from 120 to 250 km and lower-velocity layer between 80 and 120 km.

Geothermic studies have revealed low heat flow in the KC (36–38 mW·m<sup>-2</sup>), and the thermal thickness of the lithosphere has been estimated to be 200–250 km (Artemieva, 2009, 2011). The analysis of a three-dimensional (3D) P-velocity model (Tsvetkova et al., 2010, 2019) indicates that the lower boundary (the beginning of the lowered velocity zone) of the lithosphere in the central KC lies at a depth of 250–275 km.

Studies conducted using Rayleigh wave inversions (Calcagnile, 1991) have identified three velocity isolines at depths of 72, 97, and 122 km with thicknesses of 60–85, 85–110, and 110–135 km, respectively (Mitrofanov and Sharov, 1998). Near the KOS6 Station, the velocities of 8.2, 8.4, and 8.5 km·s<sup>-1</sup> have been recorded at these depths, respectively. Tomographic studies have identified the boundary of the mechanically strong lithosphere at a depth of 130 km and asthenosphere at 280 km (Sandoval et al., 2004; Hjelt et al., 2006).

Data on mantle xenoliths and xenocrysts from Proterozoic (1200 and 600 Ma) kimberlites and lamproites can be used to estimate lithospheric thickness, as well as to understand the composition and stratification of the lithosphere. The SCLM of the KC comprises spinel, spinel-garnet, and garnet peridotites; eclogite lenses have been observed infrequently among the latter two (Peltonen et al., 2002; Lehtonen et al., 2004; O'Brain et al., 2005; Peltonen and Brüggmann, 2006; Antonov and Ulianov, 2008; Lehtonen and O'Brien, 2009; Gor'kovets et al., 2013). In the western part of the craton, the lithosphere can be divided into three layers: upper - A, middle - B, and lower - C (O'Brain et al., 2005; Peltonen and Brüggmann, 2006). The A-layer comprises metasomatised fine-grained spinel, spinel-garnet, and garnet harzburgites and can be traced from the Mohorovičić discontinuity (Moho) to a depth of 110 km. The upper boundary of garnet-bearing peridotites in A-layer lies at a depth of 75–80 km. The B-layer can be traced across a depth range of 130–180 km and comprises coarse-grained garnet peridotites (lherzolites, harzburgites, and wehrlites). In this layer, the graphite–diamond equilibrium line lies at a depth of 140 km. The C-layer can be traced across a depth range of 180–240 (275) km and comprises coarse-grained fertile garnet peridotites (lherzolites) that exhibit no signs of schistosity. Diamondiferous lenses have been identified among them (Peltonen et al., 2002; Lehtonen et al., 2004; O'Brain et al., 2005). This three-layered stratification of the SCLM occurs in the western part of the KC close to its contact with the Svecofennian orogen.

The Kostomuksha kimberlite–lamproite field is located in the central part of the craton, beneath the KOS6 Station (Gor'kovets et al., 2013; Kargin et al., 2014; Gor'kovets and Sharov, 2015); the Kuhmo–Lentiira field lies 50 km to the west (Lehtonen and O'Brien, 2009) (Fig. 1). The Kostomuksha lamproites and kimberlites contain mantle xenoliths of spinel and garnet peridotites (lherzolites, harzburgites, and dunites). Low-Ca, Cr-rich pyropes of G10 type, which are typical of diamondiferous-facies harzburgites (according to the classification (Grütter et al., 2004)), are dominant among the garnet xenocrysts of the Kostomuksha field (Antonov and Ulianov, 2008; Gor'kovets et al., 2013; Gor'kovets and Sharov, 2015). Thermobarometric studies on garnet xenocrysts from the kimberlites of the Kuhmo–Lentery Group (Lehtonen and O'Brien, 2009) and on chrome-diopsides from the Kostomuksha lamproites (Antonov and Ulianov, 2008) have revealed that the lithosphere of the central KC is 250–275 km thick. Compared with the western marginal zone of the KC, the SCLM structure is more homogeneous, and the A-layer is absent. Most of the SCLM (up to 230 km) comprises depleted harzburgites and lherzolites typical of the B-layer. The C-layer lies at a depth of 230–280 km, and it is from these depths that high-Ti pyropes (G11-type) were transported, suggesting that the C-layer comprises metasomatised peridotites.

## 2.2. Geology and deep lithospheric structure of the BMB

The BMB comprises repeatedly (in both the Archean and the Paleoproterozoic) highly metamorphosed Archean (2.9–2.7 Ga) granite gneisses, metavolcanic rocks, and metasediments. It also contains scarce tectonic slices of eclogite-bearing melange, as well as Paleoproterozoic gabbro with coronitic structures, granitoids, and pegmatites (Voldichev, 1990; Glebovitsky et al., 1996; Bibikova et al., 1999, 2004; Daly et al., 2006; Slabunov, 2008; Zozulya et al., 2009; Hölttä et al., 2014; Balagansky et al., 2015; Slabunov et al., 2021); it is characterized by an overlapped fold structure (Miller and Milkevich, 1995; Sharov et al., 2010). A system of Meso-Neoproterozoic White Sea rifts extends across

the BMB from SE to NW (Baluev, 2016; Zhuravlev, 2007; Baluev et al., 2012). Devonian alkaline and kimberlite intrusions and dikes from Kola alkaline Province which marks Paleozoic plume activity exists in the northern part of the BMB (Fig. 1) (Arzamastsev et al., 2009; Zozulya et al., 2009). The foci of present high-magnitude earthquakes are in Kandalaksha Bay (Sharov, 2004), which emphasises the ongoing tectonic activity in this zone.

The deep crustal structure of the BMB has been extensively studied using deep seismic sounding and common depth point methods (Fig. 1) (Sharov, 2001, 2017). Experiments have identified that its thickness varies from 37 to 40 km (Sharov et al., 2020).

As outlined above, the structure of the upper mantle beneath the Fennoscandian Shield has been studied using the Rayleigh wave inversion method (Calcagnile, 1991); it contains three sections of velocity isolines at depths of 72, 97, and 122 km with thicknesses of 60–85, 85–110, and 110–135 km, respectively (Mitrofanov and Sharov, 1998). The following velocity variations were observed for these isolines in the BMB near the KEMI Seismic Station: 8.4, 8.2, and 8.6 km·s<sup>-1</sup>, respectively (Mitrofanov and Sharov, 1998).

Thermometric data have revealed that the lithosphere in the southern BMB is 200–250 km thick, and that the BMB–KC boundary is absent (Arzamastsev and Glaznev, 2008; Artemieva, 2009, 2011). In the northern part, close to the region of Devonian intraplate plume magmatism (Kola alkaline province), the heat flow increases to 38–46 mW·m<sup>-2</sup>, and the thermal thickness of the lithosphere decreases to 200 km. Data on the composition of garnet xenocrysts from Devonian kimberlites (Yermakovskaya pipe) and lamproites also indicate that the lithospheric thickness decreases to 140 km (Zozulya et al., 2009). The lower boundary (the beginning of a lowered velocity zone) of the lithosphere in the BMB lies at a depth of approximately 300 km, based on a 3D P-velocity tomographic models (Sandoval et al., 2004; Tsvetkova et al., 2019).

## 3. Methods

The modernised Karelian Seismological Network was used to study the crust, subcrustal lithosphere, and upper mantle using the receiver function method (Vinnik, 1977; Farra and Vinnik, 2000). This method is based on the identification of converted waves from teleseismic earthquakes and their joint inversion forming a velocity model. The model identifies the crustal and upper mantle boundaries using P- and S-wave velocity variations. This method uses converted Ps and Sp waves from teleseismic earthquakes that are transformed from P to SV (PRF modification) and from S to P (SRF modification) at seismic boundaries in the seismic station subarea.

The algorithms for obtaining PRF and SRF have been comprehensively described in previous studies (Vinnik, 1977; Farra and Vinnik, 2000). The major advantage of this method is that it can obtain 1D velocity models of Vp, Vs, and Vp/Vs distributions to a depth of 300 km based on the data from a single station. The present study regarding the lithospheric structure of the central Archean KC and western BMB was conducted using data from the KOS6 and KEMI seismic stations (Fig. 1).

In the PRF technique, earthquakes were selected from distances of 35 to 90°. Earthquakes from distances of 70 to 90° were selected in SRF modification, because the wave forms of a group of S-waves can be used for separating them into phases. The epicenters of the earthquakes used for data processing are shown in Fig. 2.

PRF and SRF are calculated using Seismic Handler software by Klaus Stammer (Seismic Handler, 2022) in the Linux operation system and the software programmes developed by the Laboratory of the Origin, Internal Structure and Dynamics of the Earth and Planets at Schmidt Institute of Physics of the Earth of the Russian Academy of Sciences.

Reference three-component broadband records with impulse onsets of P and S phases are processed using the following algorithm

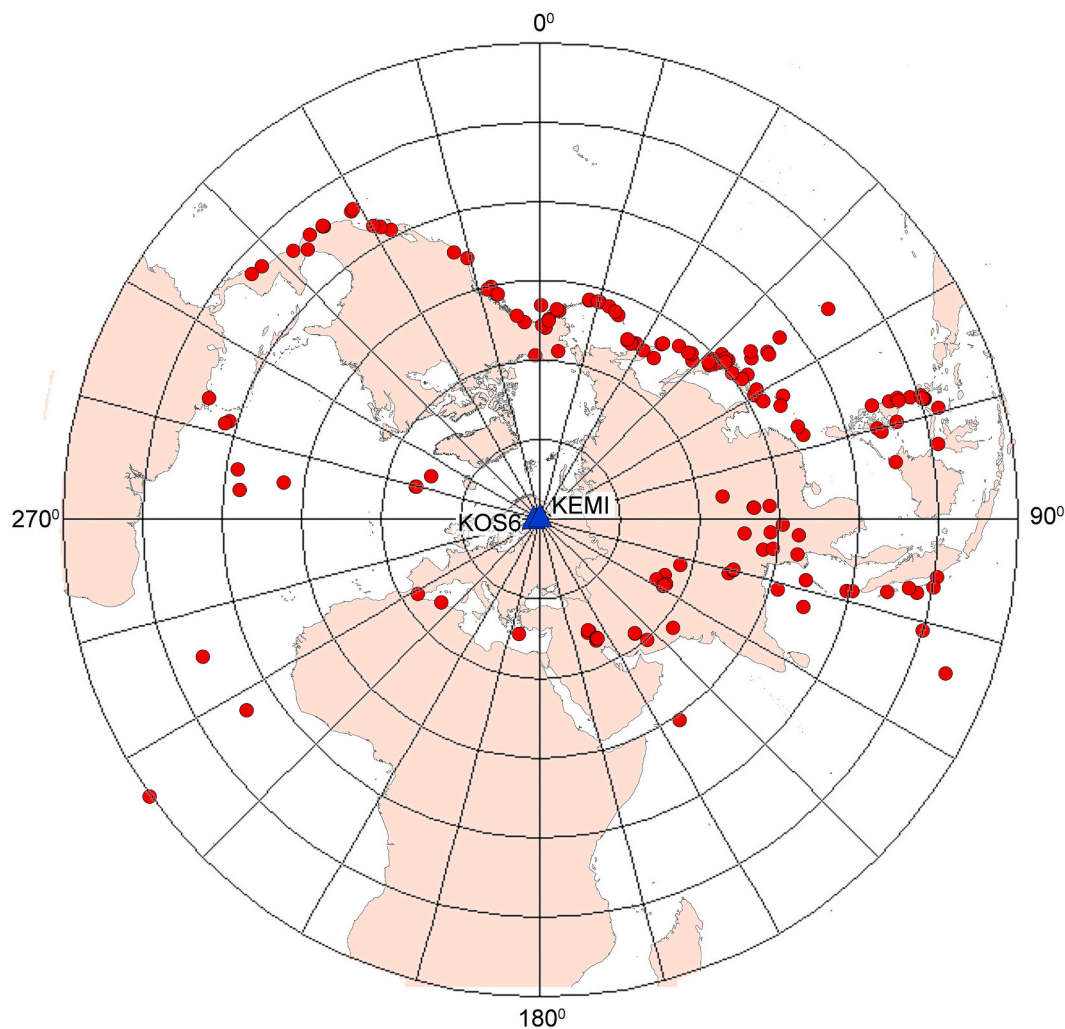


Fig. 2. Map of earthquake epicenters used for data processing.

- Frequency filtration of original records: frequency filtration in PRF modification was performed initially using a Butterworth high-pass filter HP-30-4, followed by a Butterworth low-pass filter LP-2-2. Frequency filtration in SRF modification was performed initially using a high-pass filter HP-30-2, followed by a low-pass filter LP-8-2.
  - The rotation of the reference coordinate system for the best identification of a converted wave signal: in PRF modification the Z, N, and E coordinate systems were transformed into a L, Q, and T coordinate systems. L-component was parallel to the principal direction of the particle motion in the wave propagation plane and described P-wave, Q-component was orthogonal to the main component in the same plane and was optimum for identifying Ps converted wave from the discontinuity at various depths, and T was a tangential component containing the energy of SH-wave. In SRF modification Z, N, and E coordinate systems were transformed into L, A, and B coordinate systems. A-axis corresponded to the main direction of the movement of the S particles of the wave in the propagation plane, L-axis was perpendicular to A and was optimum for identifying Sp converted phases, and B-axis was perpendicular to L- and A-axes.
  - Standardization of the resulting components for removing the effect of various source mechanisms and magnitudes: in PRF modification, standardization was performed by applying a deconvolution filter to Q-component. The filter was formed on L-component at an interval containing an incident P-wave and its code. As a result of deconvolution, standardized L-, Q-, and T-components were formed. They were receiver functions unaffected by the source and characterized the ground in the substation region. L-component had a unit amplitude, whereas Q-component had, at best, an amplitude of a few percent of it. In SRF modification, fluctuation at L-component is standardized using a deconvolution filter forming on A-component in the interval containing S-wave and its code. As a result of deconvolution, standardized L-, A-, and B-components were formed.
  - Summing standardized P-receiver functions from several earthquakes: it was performed with a time shift between the arrival time of a converted wave from each particular distance and arrival time of a converted wave from a reference distance of  $67^\circ$  and the corresponding slow velocity of  $6.4 \text{ s}^\circ$ . In SRF modification, summing was preceded by weighing each S-receiver function regarding noise intensity on the corresponding L-pathway. S-receiver functions were summed with time delays obtained as the product of two values for each source. The first value called differential slow velocity was the difference in slow velocity between Sp converted wave and parent S. The second value called differential distance was the distance between the distance of a particular earthquake and a reference distance (e.g. the average distance of all available sources). P-receiver functions and S-receiver functions were obtained after summing. They comprised the structural features under the station, including the structural characteristics of the crust and upper mantle.
- Ps converted waves appeared on the record with a delay than P-wave. The zero mark coincided with the arrival time of P-wave. Ps converted waves from the boundaries manifested themselves as a

positive amplitude impulse. The delay time depended on the depth of the boundary at which the exchange took place. The delay times from Moho at KOS6 and KEMI seismic stations were 4.6 and 4.2 s, respectively. Sp converted waves arrived earlier than S-waves and were observed as an impulse of negative polarity with some advance relative to S-wave.

### 3.1. Probabilistic joint inversion of P and S-receiver function

To model Vp and Vs velocity distributions to a depth of 300 km, total PRF and SRF pathways shown in Fig. 3 c and f are used.

Here, the short-period PRF complement the long-period SRF, so the joint inversion is efficient. The inversion methods were based on the Monte Carlo method (Kiselev et al., 2008; Vinnik et al., 2007) and are applied in the initial model comprising 10 horizontal layers lying on half-space including 4 layers in the crust and 6 layers in the mantle. This is sufficient based on our previous experience. Parameters in each layer were preset in the form of a wide range of values. Synthetic Q and L components for Ps and Sp waves, respectively, were calculated for each trial model and were compared with experimental curves. Synthetic functions were calculated using Thomson–Haskell's matrix method for flat waves and flat layers with corrections for the spherical shape of the Earth (Haskell, 1962).

A misfit function, corresponding with the smallest difference between synthetic and observed receiver functions, was calculated for each trial model. Minimization was performed using the simulated annealing method (Mosegaard & Vestergaard, 1991; Kiselev et al., 2008). This method constructs a sequence of models, converging to the misfit function minimum from four randomly selected starting points. A starting model was randomly selected within the assumed region of solutions, and each subsequent model was developed as the slight

modification of the previous one. 100,000 models are calculated during inversion. The histogram of which is shown by a colour code. To assess the ambiguity of the result, 10,000 most suitable models are saved. We divide the parameter space of the model into cells, calculate the number of coincidences in each cell and present this histogram using a colour code. The colour legend shows the number of models (from 100 to 10,000) in one or another cell. The orange and red colour shows the most reliable solutions based on the largest number of satisfying models. Less reliable solutions are shown in green and yellow. Fig. 4 shows the 1-D velocity models of the lithosphere of the central KC (below KOS6 Station) and the western BMB (below KEMI Station), on which the velocity distribution is represented by a solid black line for comparing the velocities in the model IASP91.

### 3.2. 1D velocity models of the lithosphere

Seismic data were processed using the above method to construct 1D velocity models of the lithosphere for the central KC (beneath KOS6 Station) and western BMB (beneath KEMI Station; (Fig. 4).

## 4. Results

### 4.1. KOS6 station in the KC

It was difficult to determine the boundaries beneath KOS6 Seismic Station by analysing the variations in P wave velocity (Vp) with depth. The Vp values in the crust varied from 6.7 to 7 km·s<sup>-1</sup>. The Moho, as identified by P-waves, was located at a depth of approximately 40 km. Despite the discontinuity of the velocity curve, the Vp value likely increased to 8.0 km·s<sup>-1</sup>.

The mantle only had one clear boundary, characterized by an

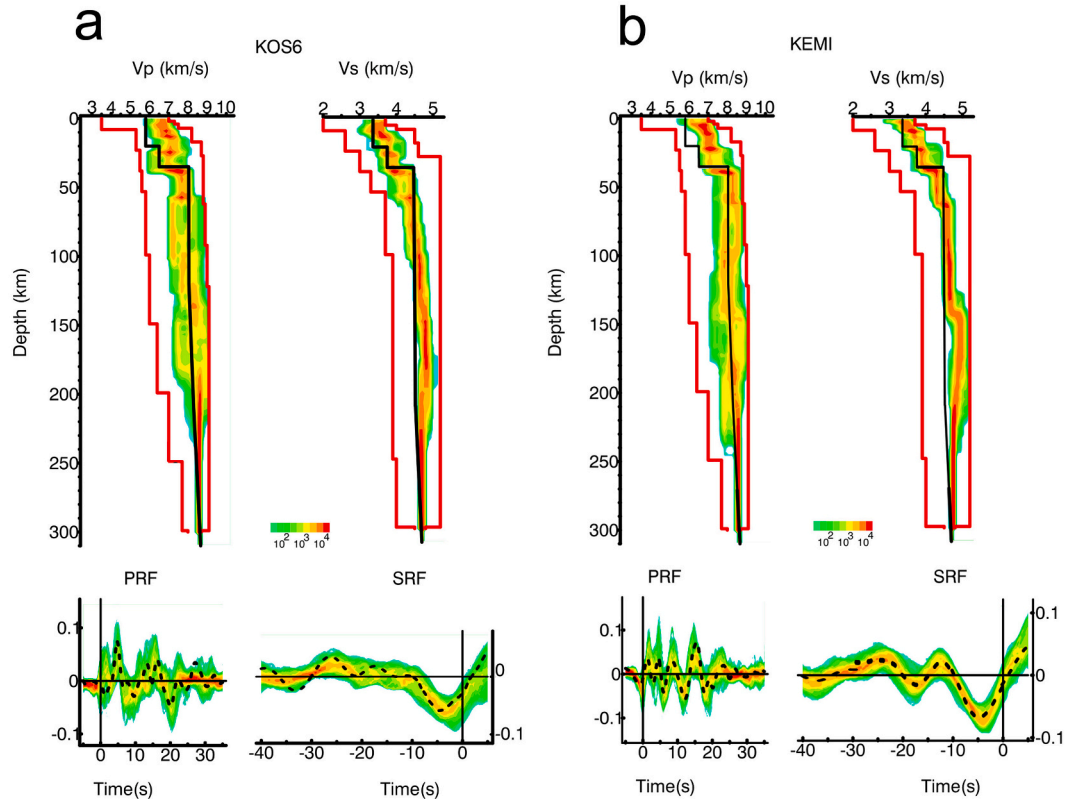


**Fig. 3.** Vp and Vs velocity models under seismic stations a) KOS6 and b) KEMI, obtained by joint inversion of PRF and SRF. Velocity models are represented by the probability density of the velocity distribution from green (less reliable values) to orange (more reliable values). Black lines on the graph show velocity distribution in accordance with the IASP91 model. The red lines show the preset velocity range limiting minimum and maximum values. Dotted black lines are observed PRF and SRF. (For interpretation of the references to colour in this figure legend, the reader is referred to the web version of this article.)

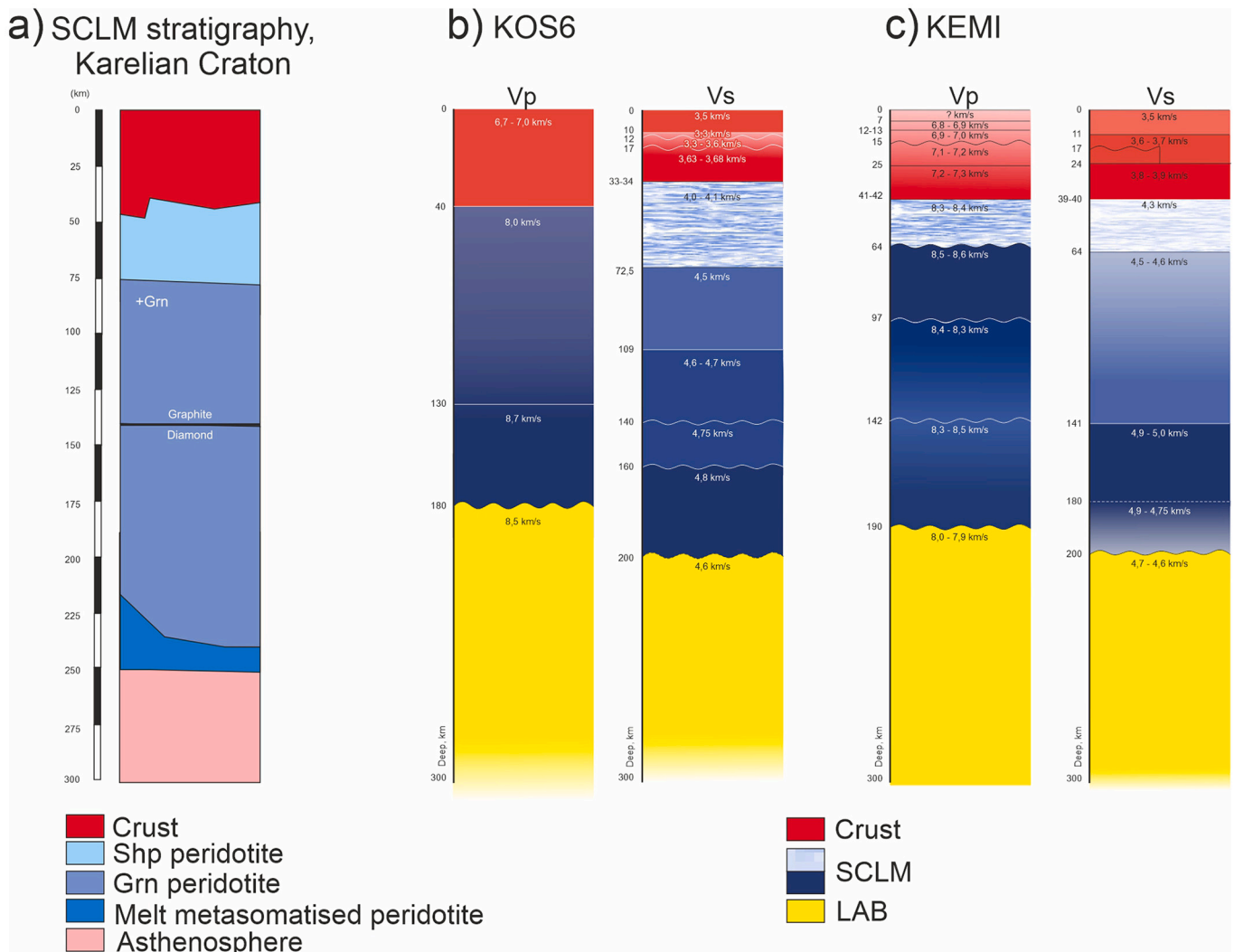


**Fig. 4.** Models of the SCLM for the central KC a) based on analysis of xenoliths and xenocrysts from kimberlites (Lehtonen and O'Brien, 2009), and 1-D velocity models of the lithosphere of b) the KC - KOS6 Seismic Station and c) the BMB - KEMI Seismic Station; b) and c) are based on data obtained using the receiving function method.

increase in  $V_p$  from 8.0 to 8.7  $\text{km}\cdot\text{s}^{-1}$  at a depth of 130 km. This boundary was likely associated with the variations in the mantle composition. P wave velocity at a depth of 130–180 km reached a maximum of 8.7–8.8  $\text{km}\cdot\text{s}^{-1}$ .  $V_p$  gradually decreased from 8.5  $\text{km}\cdot\text{s}^{-1}$  at a depth of 180 km and continued decreasing until a depth of 300 km (Fig. 5 a). This type of variation in the velocity parameters, with maximum values at a depth of 100–150 km followed by a gentle decrease, is typical for the lithosphere of many old cratons (Artemieva, 2011).

The shear waves ( $V_s$ ) velocities in the crust were clear, while intracrustal boundaries, as with the P wave velocity model ( $V_p$ ), were difficult to define (Fig. 4 a). The intracrustal boundaries for  $V_s$  were from 3.3 to 3.5  $\text{km}\cdot\text{s}^{-1}$  at a depth of 10 km and from 3.5 to 3.7  $\text{km}\cdot\text{s}^{-1}$  in the depth range of 16–20 km.  $V_s$  increased rapidly from 3.7 to 4–4.1  $\text{km}\cdot\text{s}^{-1}$  at a depth of 33–34 km, indicating the Moho. The transverse wave distribution velocity from the Moho to a depth of 72.5 km was 4–4.1  $\text{km}\cdot\text{s}^{-1}$  (Fig. 4 a). At a depth of 72.5 km, the  $V_s$  exhibited a sharp boundary, with an increase in velocity from 4.1 to 4.5  $\text{km}\cdot\text{s}^{-1}$ . The  $V_s$  value (4.5  $\text{km}\cdot\text{s}^{-1}$ ) was the same for all mantle rocks across the depth interval of 72.5–109 km. At depths of 109, 140, and 160 km,  $V_s$  values increased in a stepwise manner from 4.5 to 4.6–4.7  $\text{km}\cdot\text{s}^{-1}$ , from 4.7 to 4.75  $\text{km}\cdot\text{s}^{-1}$ , and from 4.75 to 4.8  $\text{km}\cdot\text{s}^{-1}$ , respectively.  $V_s$  values remained in the 160–200 km range (maximum of 4.8  $\text{km}\cdot\text{s}^{-1}$ ), and according to the velocity model,  $V_s$

values decreased from a depth of 200 km (Fig. 4a).

The following stratification was determined based on the analysis of variations in P and S wave velocities in the lithosphere of the central KC (Fig. 4a):

- 33–40 km thick crust; its boundary with the mantle (Moho) was marked by a rapid velocity change ( $V_p$  from 7.0 to 8.0  $\text{km}\cdot\text{s}^{-1}$  and  $V_s$  from 3.7 to 4–4.1  $\text{km}\cdot\text{s}^{-1}$ ), typical for the material composition change.
- ~40 km thick layer in the upper mantle structure from the Moho to 72.5 km depth, as identified from the  $V_s$  model as having a velocity of 4–4.1  $\text{km}\cdot\text{s}^{-1}$ . The boundary at the bottom of this layer is sharp, likely associated with the changes in mantle composition.
- 60–70 km thick layer in the mantle structure at a depth of 72.5–140 (130) km, as identified by the changes in  $V_s$  (4.5–4.75  $\text{km}\cdot\text{s}^{-1}$ ) and  $V_p$  (8.0  $\text{km}\cdot\text{s}^{-1}$ ). The  $V_p$  model shows that at a depth of ~130 km, velocity increased rapidly from 8.0 to 8.7  $\text{km}\cdot\text{s}^{-1}$ , whereas a gradual increase in velocity was observed at a depth of ~140 km. This boundary is likely associated with phase transitions in mantle composition.
- ~50–60 km thick layer in the depth range of (130) 140–(180) 200 km. A zone of maximum  $V_s$  (4.8  $\text{km}\cdot\text{s}^{-1}$ ) and  $V_p$  (8.7  $\text{km}\cdot\text{s}^{-1}$ ) values was identified at a depth of 160–200 km.

- Velocities began decreasing from a depth of 180–200 km, according to the IASP91 model values.

The lithosphere–asthenosphere boundary (LAB) was undetermined.

#### 4.2. KEMI station in the BMB

Vp values were estimated from the velocity model obtained (Fig. 4b) from a depth of 7 km: 6.8–6.9 km·s<sup>-1</sup>. The velocity increased gradually in the crust: 12–13 km by 6.9–7.0 km·s<sup>-1</sup>; 15 km by 7.1–7.2 km·s<sup>-1</sup>, and 25 km by 7.2–7.3 km·s<sup>-1</sup>. The velocity remained constant from a depth of 25 km to the Moho (41 km) at approximately 7.3 km·s<sup>-1</sup>.

The Moho was clearly indicated by a rapid increase in Vp from 7.3 to 8.3–8.4 km·s<sup>-1</sup> at a depth of 41–42 km. The Vp value (8.3–8.4 km·s<sup>-1</sup>) remained constant from the Moho to a depth of 64 km. At a depth of 64 to 97 km, the Vp ranged from 8.5 to 8.6 km·s<sup>-1</sup>. Across the depth range of 97–142 km, the Vp value decreased to 8.3–8.4 km·s<sup>-1</sup> relative to the overlying and underlying horizons. Vp was determined to be unreliable at a depth of 142–190 km; however, Vp tended to increase relative to the overlying horizon. Over a depth of 190 km, Vp decreased to 8.0–7.9 km·s<sup>-1</sup>. The obtained velocity model was difficult to interpret because of the poorly defined Vp values.

The Vs model at the KEMI Station (Fig. 4b) exhibited better-defined characteristics. Therefore, these data could be analysed more reliably. Vs was 3.5 km·s<sup>-1</sup> up to a depth of 11 km, where the first intracrustal boundary was detected, as indicated by a jump in Vs from 3.5 to 3.7 km·s<sup>-1</sup>. The next boundary in the crust was identified at a depth of 24 km, as demonstrated by an increase in Vs to 3.9 km·s<sup>-1</sup>. The Moho was identified by a rapid increase in velocity (to 4.3 km·s<sup>-1</sup>) at a depth of 39–40 km. In the upper mantle from the Moho to 64 km, Vs was estimated to be 4.3 km·s<sup>-1</sup>. At depth of 64 km, Vs increased rapidly to 4.5–4.6 km·s<sup>-1</sup>. These values (Vs 4.5–4.6 km·s<sup>-1</sup>) remained constant in the depth range 64–141 km; in contrast to Vp, Vs gradually increased here. At a depth of 141 km, Vs increased sharply from 4.5 to 4.6 to 4.9–5.0 km·s<sup>-1</sup>. These Vs values are typical of a ~40 km thick layer (in the 141–180 km range), and they were the highest values calculated by the model. Vs decreased gradually from 4.9 to 5.0 to 4.9–4.75 km·s<sup>-1</sup> in the depth range of 180–200 km. From a depth of 200 km, Vs reached 4.7–4.6 km·s<sup>-1</sup>, based on the IASP91 model.

The lithosphere of the western BMB was also stratified (Fig. 4b) and comprised the following:

- 39–42 km thick crust. Its boundary with the mantle (Moho) was clearly indicated by a sharp change in velocity parameters (Vp from 7.3 to 8.3–8.4 km·s<sup>-1</sup> and Vs from 3.9 to 4.3 km·s<sup>-1</sup>). This was caused by the variations in rock composition at the Moho;
- ~25 km layer in the upper mantle from the Moho to 64 km with velocity characteristics (Vp 8.3–8.4 km·s<sup>-1</sup>, Vs – 4.3 km·s<sup>-1</sup>) higher than those of the IASP91 model for Vp but lower for Vs. The boundary at the base of this layer was likely associated with the variations in mantle composition;
- 30 km thick layer in the upper mantle in the depth range of 64–97 km. Its velocity parameters (Vs 4.5–4.6 km·s<sup>-1</sup> and Vp 8.5–8.6 km·s<sup>-1</sup>) were higher than those of the IASP91 model;
- 45 km thick layer in the depth range of 97–142 km with lower velocities for Vp (8.4–8.3 km·s<sup>-1</sup>); this layer was associated with the observed variations in the velocity characteristics of the mantle and their anomalously low velocity values in this depth range (After Mitrofanov and Sharov, 1998);
- 60 km thick layer in the depth range of 141–200 km with the highest Vp values (at least 8.3–8.5 km·s<sup>-1</sup>). Within this layer, a layer (141–180 km) with highest Vs values of 4.9–5.0 km·s<sup>-1</sup> was delineated. At the base of this layer, at a depth of 180–200 km, a zone was detected where Vs and Vp decreased gradually from 4.9 to 5.0 to 4.9–4.75 km·s<sup>-1</sup> and 8.3–8.5 to 8.0–7.9 km·s<sup>-1</sup>, respectively.

At depths over 200 km, the velocity characteristics of the mantle (Vp 8.0 km·s<sup>-1</sup> and Vs 4.6 km·s<sup>-1</sup>) were consistent with those predicted by the IASP91 model. A zone of lower velocity, which could have been interpreted as LAB, was not revealed.

Thus, similar to the KC, the mantle beneath the BMB exhibited a clear upper boundary but no well-defined lower distinct stratification at the lower boundary. This was indicated by the variations in its velocity characteristics, for example, the maximum velocity values in the middle part of mantle.

By generalising the description of the velocity models obtained for KOS6 and KEMI seismic stations, the lithospheric structure evidently comprised the crust and mantle, separated by the Moho. Consequently, the SCLM exhibited the following stratification:

- An upper layer that is 40 and 25 km thick in the KC and BMB, respectively;
- A middle layer that is 70 and 80 km thick in the KC and BMB. There also exists a 45 km thick decrease velocity zone in the BMB;
- A lower layer that is ~60 km thick in both the KC and BMB;
- A transitional layer (from a depth of 180–200 km in the KC and 190–200 km in the BMB) from the SCLM to asthenosphere; its thickness is unknown;
- A layer with maximum seismic velocity values (Vp and Vs) at a depth of 160–180 and 140–180 km in the KC and BMB, respectively. The velocity characteristics of lithospheric horizons of the same type in the two studied structures were different, likely due to the differences in their composition and structure.

#### 5. Discussion

The deep structure of Fennoscandian Shield by receiver functions technique was described in detail in a few previous studies (Hjelt et al., 2006; Kozlovskaya et al., 2008). 1-D model for western KC in station JOF (Vinnik et al., 2007) are different from central KC in station KOS6. There are high-velocity layers from 40 to 80 km in JOF, but decrease-velocity layers from 33 to 72.5 km in KOS6. Studies are also known a 3-D model of shear velocities in the upper crust beneath northern Finland (Poli et al., 2013) that we can use for inversion in the future.

Kuhmo–Lentiira (Lehtonen et al., 2004) and Kostomuksha (Antonov and Ulianov, 2008; Gor'kovets et al., 2013) kimberlites and lamproites are known to contain xenoliths of spinel peridotites (Lehtonen et al., 2004; Lehtonen and O'Brien, 2009; Gor'kovets et al., 2013). According to thermometric research of Riphean (1.2 Ga) Kuhmo–Lentiira kimberlites and lamproites (Lehtonen et al., 2004), garnet phenocrysts were exhumed from a depth of 75–275 km. This implies that the lithosphere here has a thickness of at least 275 km. The shallow garnet xenocrysts in Kuhmo–Lentiira kimberlites were exhumed from a depth of 75–80 km and were found to be in equilibrium with garnet–spinel-facies lherzolites (Lehtonen et al., 2004). This suggests that the upper (35–72.5 km range) craton mantle layer, with Vs of 4.0–4.1 km·s<sup>-1</sup> and Vp of 8.0 km·s<sup>-1</sup>, comprises spinel peridotites. Moreover, the rapid change in velocity values observed at a depth of 72.5 km in the KC is associated with their transition to garnet–spinel facies.

Garnet samples from Kuhmo–Lentiira kimberlites from a depth of <110 km are only associated with garnets exhibiting G9 type equilibrium with lherzolites. Garnets from a depth of over 100 km are associated with G9 and G10 types. G10 type is an indicator of harzburgite mantle composition.

The velocity increase at a depth of 110 km observed in the KOS6 velocity model could be associated with a change in mantle composition, such as a transition from a lherzolitic mantle to a lherzolitic mantle with harzburgite lenses; thus, a 115 km thick layer composed of garnet peridotites (lherzolites and harzburgites) may be present in the 110–225 km depth. This layer exhibited a graphite–diamond transition boundary at a depth of approximately 140 km. Garnet xenocrysts from these depths contained high-Ti pyrope varieties (G11 type), marking Ti-

metasomatism. Apparently, the boundary at a depth of 130–140 km, where both  $V_s$  and  $V_p$  were increasing, could be associated with the onset of metasomatic alterations in the composition of mantle peridotites and a graphite–diamond phase transition (Figs. 3 and 4).

The proportion of garnets from metasomatically altered peridotites (G11 type) among the xenocrysts of lherzolitic (G9) and harzburgitic (G10) garnets were increased rapidly from a depth of 175–180 km. The garnets of G1 type (Low-Cr, Fe-Ti-enriched megacrysts) were also observed. A decrease in  $V_p$  and  $V_s$  in the 180–200 km range was associated with an increase in the proportion of metasomatically altered peridotite and a decrease in its magnesium content. The lower part of the mantle, at a depth of 225–275 km, comprised metasomatised mantle peridotites, as indicated by high-Ti pyrope xenocrysts (G11 type) from Lentiira kimberlites exhumed from these depths.

Thus, here the 1D velocity model of the lithosphere in the central part of the KC was correlated with its stratification based on the compositional analysis of garnet xenocrysts and mantle xenoliths from the Kuhmo–Lentiira kimberlites sampled in the Kostomuksha and Kaava–Kuopio areas.

The comparison of deep velocity models of the SCLM in the BMB and KC revealed the following similarities:

- The lithosphere of both structures was at least 200 km thick;
- The lithosphere was stratified (with distinct upper, middle, and lower layers);
- The lithosphere velocity models of the BMB and KC also exhibited similar velocity variations:  $V_p$  in the BMB varied from 8.3 to 8.5  $\text{km}\cdot\text{s}^{-1}$ , whereas that in the KC varied from 8.0 to 8.7  $\text{km}\cdot\text{s}^{-1}$ ;  $V_s$  in the BMB varied from 4.3 to 5.0  $\text{km}\cdot\text{s}^{-1}$ , whereas that in the KC it varied from 4.0 to 4.8  $\text{km}\cdot\text{s}^{-1}$ ;
- The layers with maximum velocity occurred at depths of 160–180 and 140–180 (190) km in the KC and BMB, respectively;
- The Moho in both structures exhibited a roughly equal contrast, as indicated by an increase in  $V_p$  and  $V_s$  by 1 and 0.4  $\text{km}\cdot\text{s}^{-1}$ , respectively.

However, the two areas exhibited some essential structural differences:

- The thickness of the BMB crust was slightly greater (39–42 km) than that of the investigated part of the KC (33–40 km). The depth of the Moho predicted by the KOS6  $V_s$  model differed from that of the KOS6  $V_p$  model and previous studies (Sollogub, 1987; Mitrofanov and Sharov, 1998; Gorkovets and Sharov, 2015);
- The lower crust of the BMB was characterized by a considerably greater velocity ( $V_p$  values in the BMB and KC were 7.2–7.3 and < 7.0  $\text{km}\cdot\text{s}^{-1}$ , respectively;  $V_s$  values in the BMB and KC were 3.8–3.9 and 3.63–3.68  $\text{km}\cdot\text{s}^{-1}$ , respectively);
- The upper layer of the mantle in BMB was thinner and had higher velocities ( $V_s = 4.3 \text{ km}\cdot\text{s}^{-1}$  and  $V_p = 8.3\text{--}8.4 \text{ km}\cdot\text{s}^{-1}$  compared to 4.0–4.1 and 8.0  $\text{km}\cdot\text{s}^{-1}$ , respectively) than the KC. This high mantle velocity indicated that the spinel peridotites in the BMB had higher magnesium contents than those in the KC;
- The BMB mantle contained a ~ 45 km thick layer with lower  $V_p$  velocities (it is not manifested in the  $V_s$  values) at a depth of 97–142 km. A decrease in velocity at a depth of 97–122 km was also observed in a previous study conducted using the Rayleigh wave inversion method (Calcagnile, 1991). This could be associated with the tectonic layering of the mantle's garnet peridotites, leading to anisotropy resulting from the preferential orientation of olivine and pyroxene. (Babushka, 1984; Artemieva, 2011). The discussed lowered velocity zone could be associated with mantle deformations that occurred during Palaeoproterozoic collisions, which are well-defined in the crustal complexes of BMB.

Thus, the lithospheric thicknesses of the Archean KC and

Precambrian BMB are both 200 km (Tsvetkova et al., 2010, 2019) (and even 275 km, based on data from mantle xenoliths and xenocrysts). This thickness is a distinctive feature of Archean structures (Artemieva, 2011).

Notably, during Paleoproterozoic collisional processes, the Archean SCLM of the BMB was not destroyed, similar to Precambrian mobile belts (e.g. Limpopo and Anabara) (Rosen et al., 2005; Artemieva, 2009; Pedersen et al., 2006). Moreover, the lithosphere of BMB was not destroyed during the formation of the Riphean rift-related structure of the White Sea. The Paleozoic Kola mantle plume activity only destroyed the northern part of the BMB lithosphere (Zozulya et al., 2009).

1D velocity models of the lithosphere in the central part of the KC and western BMB is different with velocity models of the Kaapvaal, Zimbabwe Cratons and Limpopo Mobile Belt (Fig. 6). The upper part of the SCLM in South African cratons (50–100 km) has higher velocities, the central part of the KC and western BMB at the same depth has decrease velocities.

The velocity in the 1-D models central part of the KC and western BMB is higher in the depth range of 150–180 km than those of the in South African cratons models (Li and Burke, 2006; Pedersen et al., 2006).

However, the history of formation for the above Precambrian structures is the same (Lubnina and Slabunov, 2011). They formed in the Archean, has been activities in the Paleoproterozoic and mantle plumes in the Phanerozoic. Thus, similarity of formation history does not imply similarity in structure SCLM.

The 1D velocity models of the Archean segment of the Fennoscandian Shield lithosphere (Fig. 5) revealed a thickness of at least 200 km, whereas data from mantle xenoliths suggested no <250–275 km thickness. As discussed above, such a thick SCLM is the characteristic of Archean cratons and associated mobile belts and is corresponding with the definition of a mantle keel.

## 6. Conclusions

Here, seismic research into the lithosphere of the eastern Fennoscandian Shield, conducted using the receiver functions method, determined that the thicknesses of the central KC and western BMB are both at least 200 km, as similar research (Tsvetkova et al., 2010, 2019). The lithospheric mantle exhibited a distinct contrasting upper boundary with the crust in both structures, but its boundary with the asthenosphere was not identified in this study. For both structures, The SCLM

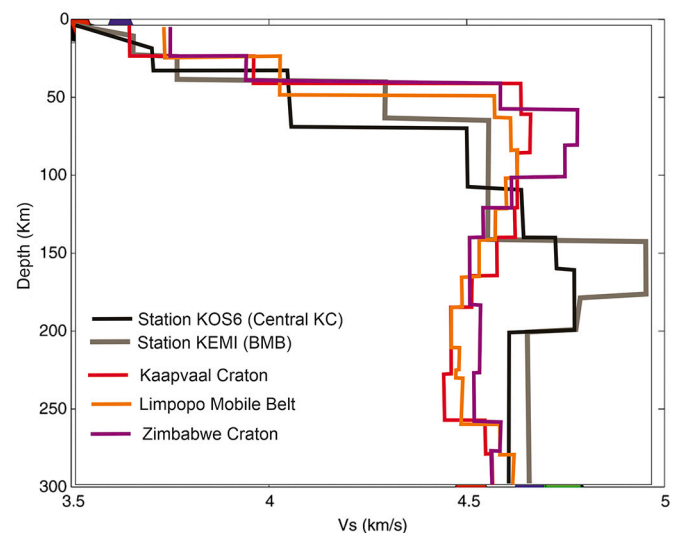


Fig. 5. One-dimensional shear wave velocity in central KC (KOS6) and BMB (KEMI). Shear wave profiles in the Kaapvaal, Zimbabwe Cratons and Limpopo Mobile Belt are plotted for comparison (Li and Burke, 2006).

was found to consist of upper, middle and lower layers. The boundary between the upper and middle layers lies at a depth near the upper line of garnet stability limit in mantle peridotites, and the boundary between the middle and lower layers corresponds to the graphite/diamond equilibrium line.

The SCLM of the BMB was shown to exhibit a distinctive zone of lower velocity within in the middle layer. The 1D velocity model of the central KC was found to be in good agreement with the evidence for the SCLM stratigraphy obtained by analysing mantle xenoliths and xenocrysts from kimberlites and lamproites from this area.

a - initial three-component records with P-phase arrival, b - individual P-receiver functions of an individual earthquake, c - total P-receiver functions of several earthquakes, d - initial three-component records with S-phase arrival, e - individual S-receiver functions of an individual earthquake, f - total S-receiver functions of several earthquakes.

## Funding

The paper has been prepared in the framework of research projects of the Karelian Research Center of the RAS AAAA-A18-118020290086-1, AAAA-A18-118020290085-4 and by projects no. 122011300389-8 of FECIAR UrB RAS.

## Declaration of Competing Interest

The authors declare that they have no known competing financial interests or personal relationships that could have appeared to influence the work reported in this paper.

## Acknowledgements

The authors are grateful to Dr. N.V. Sharov (1933-2022) for organizing scientific research. Thanks to the two anonymous reviewers and editors for their insightful comments and suggestions that greatly helped improve this article.

## References

- Antonov, A., Ulianov, A., 2008. The lithospheric mantle beneath the Central Karelia: xenoliths from the Kostomuksha lamproites/kimberlites2. In: 9th International Kimberlite Conference, Frankfurt, Germany, Extended Abstracts, No. 9IKC-A-00351. <https://doi.org/10.1016/j.gca.2006.06.050>.
- Artemieva, I.M., 2006. Global  $1^\circ \times 1^\circ$  thermal model TCI for the continental lithosphere: Implications for lithosphere secular evolution. *Tectonophysics* 416, 245–277. <https://doi.org/10.1016/j.tecto.2005.11.022>.
- Artemieva, I.M., 2009. The continental lithosphere: Reconciling thermal, seismic, and petrologic data. *Lithos* 109, 23–46. <https://doi.org/10.1016/j.lithos.2008.09.015>.
- Artemieva, I., 2011. *The Lithosphere. An Interdisciplinary Approach*. Cambridge University Press, p. 794. ISBN (Print) 978-0-521-84396-6 ISBN (Electronic) 9780511975417.
- Artemieva, I.M., Mooney, W.D., 2001. Thermal structure and evolution of Precambrian lithosphere: a global study. *J. Geophys. Res.* 106, 16387–16414. <https://doi.org/10.1029/2000JB900439>.
- Artemieva, I.M., Thybo, H., Kaban, M.K., 2006. Deep Europe today: Geophysical synthesis of the upper mantle structure and lithospheric processes over 3.5 Ga. *Geol. Soc. Lond. Mem.* 32, 11–41. <https://doi.org/10.1144/GSL.MEM.2006.032.01.02>.
- Arzamastsev, A.A., Glaznev, V.N., 2008. Plume-lithosphere interaction in the presence of an ancient sublithospheric mantle keel: an example from the Kola Alkaline Province. *Dokl. Earth Sci.* 419, 384–387. <https://doi.org/10.1134/S1028334X08030069>.
- Arzamastsev, A.A., Fedotov, Zh.A., Arzamastseva, L.V., 2009. Dyke magmatism of the North-Eastern part of the Baltic Shield. SPb.: Nauka 383 p. ISBN: 978-5-02-025361-2.
- Babushka, V., 1984. P wave velocity anisotropy in crystalline rocks. *Geophys. J.R. Astron. Soc.* 76, 113–119.
- Balagansky, V., Shchipansky, A., Slabunov, A., Gorbunov, I., Mudruk, S., Sidorov, M., Azimov, P., Egorova, S., Stepanova, A., Voloshin, A., 2015. Archean Kuru-Vaara eclogites in the northern Belomorian Province, Fennoscandian Shield: crustal architecture, timing and tectonic implications. *Int. Geol. Rev.* 57, 1543–1565. <https://doi.org/10.1080/00206814.2014.958578>.
- Baltysbaev, Sh.K., 2013. Svecofennian orogen of the fennoscandian shield: compositional and isotopic zoning and its tectonic interpretation. *Geotectonics* 47, 452–464. <https://doi.org/10.1134/S0016852113060022>.
- Baluev, A.S., 2016. Geodynamics of the riphean stage in the evolution of the northern passive margin of the East European craton. *Geotectonics* 40, 183–196. <https://doi.org/10.1134/S0016852106030034>.
- Baluev, A.S., Zhuravlev, V.A., Terekhov, E.N., Przhivalgovsky, E.S., 2012. Tectonics of the White Sea and Adjacent Territories (Explanatory note to the “Tectonic map of the White Sea and adjacent territories” scale 1: 1500000). GEOS, Moscow, p. 104 (ISSN 0002-3272).
- Bibikova, E.V., Slabunov, A.I., Bogdanova, S.V., Sheld, T., Stepanov, V.S., Borisova, E. Yu., 1999. Early magmatism of the Belomorian mobile belt, Baltic shield: lateral zoning and isotopic age. *Petrology* 7, 123–146. ISSN: 0869-5911.
- Bibikova, E.V., Bogdanova, S.V., Glebovitsky, V.A., Claesson, S., Skjöld, T., 2004. Evolution of the Belomorian Belt: NORDSIM U-Pb Zircon dating of the Chupa Paragneisses, magmatism and metamorphic stages. *Petrology* 12, 195–210. ISSN: 0869-5911.
- Bogatikov, O.A., Kononova, V.A., Nosova, A.A., Kondrashov, I.A., 2007. Kimberlites and lamproites of the East European Platform. *Petrol. Geochem. Petrol.* 15, 315–334. <https://doi.org/10.1134/S0869591107040017>.
- Calcagnile, G., 1991. Deep structure of Fennoscandia from fundamental and higher mode dispersion of Rayleigh waves. *Tectonophysics* 195, 139–149. [https://doi.org/10.1016/0040-1951\(91\)90209-B](https://doi.org/10.1016/0040-1951(91)90209-B).
- Daly, J.S., Balagansky, V.V., Timmerman, M.J., Whitehouse, M.J., 2006. The Lapland-Kola Orogen: palaeoproterozoic collision and accretion of the northern Fennoscandian lithosphere. *Geol. Soc. Lond. Mem.* 32, 579–598. <https://doi.org/10.1144/GSL.MEM.2006.032.01.35>.
- Farra, V., Vinnik, L., 2000. Upper mantle stratification by P and S receiver functions. *Geophys. J. Int.* 141, 699–712. <https://doi.org/10.1046/j.1365-246x.2000.00118.x>.
- Glebovitsky, V.A., 2005. Ex. Ed. Early Precambrian of the Baltic Shield. Saint Petersburg: Nauka, p. 711. ISBN: 5-02-024950-5.
- Glebovitsky, V.A., Miller, Yu.V., Drugova, G.M., Milkevich, R.I., Vrevsky, A.B., 1996. Structure and metamorphism of the Belomorian-Lapland collision zone. *Geotectonics* 30, 53–63. ISSN: 0016-8521.
- Glushanin, L.V., Sharov, N.V., Shchiptsov, V.V. (Eds.), 2011. *Palaeoproterozoic Onega Structure (Geology, Tectonics, Deep Structure and Mineralogy)*. KarRC RAS, Petrozavodsk, p. 431. Ex. Ed. ISBN: 978-5-9274-0456-8.
- Gorkovets, V.Ya., Sharov, N.V. (Eds.), 2015. *Kostomuksha Ore Area (Geology, Deep Structure and Mineralogy)*. KarRC RAS, Petrozavodsk, p. 322. ISBN: 978-5-9274-0668-5.
- Gorkovets, V. Ya, Rudashevskii, N.S., Rudashevsky, V.N., Antonov, A.V., 2013. Indicator minerals of diamond in the lamproitic diatreme, Kostomuksha region, Karelia. *Dokl. Earth Sci.* 450, 62–65. <https://doi.org/10.1134/S1028334X13050024>.
- Griffin, W.L., O'Reilly, S.Y., 2019. The earliest subcontinental lithospheric mantle earth's. In: van Kranendonk, M.J., Bennett, V.C., Hoffmann, J.E. (Eds.), *Oldest Rocks*, Second edition. Elsevier, pp. 81–102. [https://doi.org/10.1016/S0166-2635\(07\)15082-9](https://doi.org/10.1016/S0166-2635(07)15082-9).
- Griffin, W.L., O'Reilly, S.Y., Abe, N., Aulbach, S., Davies, R.M., Pearson, N.J., Doyle, B.J., Kivi, K., 2003. The origin and evolution of Archean lithosphere mantle. *Precambrian Res.* 127, 19–41. [https://doi.org/10.1016/S0301-9268\(03\)00180-3](https://doi.org/10.1016/S0301-9268(03)00180-3).
- Grütter, H.S., Gurney, J.J., Menzies, A.H., Wintera, F., 2004. An updated classification scheme for mantle-derived garnet, for use by diamond explorers. *Lithos* 77, 841–857. <https://doi.org/10.1016/j.lithos.2004.04.012>.
- Haskell, N.A., 1962. Crustal reflection of plane P and SV waves. *J. Geophys. Res.* 67, 4751–4767. <https://doi.org/10.1029/JZ067i012p04751>.
- Hjelt, S.E., Korja, T., Kozlovskaya, E., Lahti, I., Yliniemi, J., 2006. Electrical conductivity and seismic velocity structures of the lithosphere beneath the Fennoscandian Shield. In: BEAR Working Group and SVEKALAPKO Seismic Tomography Working Group, Geological Society, London, Memoirs, 32, pp. 541–559. <https://doi.org/10.1144/GSL.MEM.2006.032.01.33>.
- Hölttä, P., Heilimo, E., Huhma, H., Kontinen, A., Mertanen, S., Mikkola, P., Paavola, J., Peltonen, P., Semprich, J., Slabunov, A., Sorjonen-Ward, P., 2012. The Archaean of the Karelia Province in Finland. In: *Geological Survey of Finland. Special Paper* 54, pp. 21–73. [http://arkisto.gtk.fi/sp/sp\\_054.pdf](http://arkisto.gtk.fi/sp/sp_054.pdf) (ISBN 978–952–217-213-6 (pdf) ISSN: 0782-8535).
- Hölttä, P., Heilimo, E., Huhma, H., Kontinen, A., Mertanen, S., Mikkola, P., Paavola, J., Peltonen, P., Semprich, J., Slabunov, A., Sorjonen-Ward, P., 2014. The Archaean Karelia and Belomorian Provinces, Fennoscandian Shield. In: Dilek, Y., Furnes, H. (Eds.), *Evolution of Archean Crust and Early Life. 7. Modern Approaches in Solid Earth Sciences*, pp. 55–102. [https://doi.org/10.1007/978-94-007-7615-9\\_3](https://doi.org/10.1007/978-94-007-7615-9_3).
- Kargin, A.V., Nosova, A.A., Larionova, Y.O., Kononova, V.A., Borisovsky, S.E., Kovalchuk, E.V., Griboedova, I.G., 2014. Mesoproterozoic Orangeites (Kimberlites II) of West Karelia: mineralogy, geochemistry, and Sr–Nd isotope composition. *Petrology* 22, 151–183. <https://doi.org/10.1134/S0869591114020039>.
- Khain, V.E., 2003. The main problems of modern geology. In: M.: Scientific World, p. 348 [In Russian] ISBN 5-89176-218-8.
- Kiselev, S., Vinnik, L., Oreshin, S., Gupta, S., Rai, S.S., Singh, A., Kumar, M.R., Mohan, G., 2008. Lithosphere of the Dharwar craton by joint inversion of P and S receiver functions. *Geophys. J. Int.* 173, 1106–1118. <https://doi.org/10.1111/j.1365-246X.2008.03777.x>.
- Kozlovskaya, E., Kosarev, G., Aleshin, I., Riznichenko, O., Sanina, I., 2008. Structure and composition of the crust and upper mantle of the Archean–Proterozoic boundary in the Fennoscandian shield obtained by joint inversion of receiver function and surface wave phase velocity of recording of the SVEKALAPKO array. *Geophys. J. Int.* 175, 135–152. <https://doi.org/10.1111/j.1365-246X.2008.03876.x>.
- Kukkonen, I.T., Peltonen, P., 1999. Xenolith-controlled geotherm for the central Fennoscandian Shield: implications for lithosphere–asthenosphere relations. *Tectonophysics* 304, 301–315. [https://doi.org/10.1016/S0040-1951\(99\)00031-1](https://doi.org/10.1016/S0040-1951(99)00031-1).

- Kulikov, V.S., Svetov, S.A., Slabunov, A.I., Kulikova, V.V., Polin, A.K., Golubev, A.I., Gorkovets, V. Ya, Ivashchenko, V.I., Gogolev, M.A., 2017. Geological map of southeastern Fennoscandia (scale 1:750 000): a new approach to map compilation. In: Transactions of the KarRC RAS, Precambrian Geology Series, 2, pp. 3–41. <https://doi.org/10.17076/geo444>.
- Lahtinen, R., Garde, A.A., Melezchik, V.A., 2008. Paleoproterozoic evolution of Fennoscandia and Greenland. Episodes 31, 1–9. <https://doi.org/10.18814/epiugs/2008/v31i1/004>.
- Lebedev, A.A., Meshcheryakova, V.A., 2014. Spectral characteristics of seismic noise in the Karelian network of seismological stations. In: Proceedings of the XIX Scientific-Practical Conference with International Participation "Active Faults and their Importance for the Assessment of Seismic Hazard: The Current State of the Problem." IPC "Scientific Book", Voronezh, pp. 207–209. ISBN 978-5-4446-0509-7. [http://www.gsr.ru/new/public/books/2014/Razlomy\\_9-conf.pdf](http://www.gsr.ru/new/public/books/2014/Razlomy_9-conf.pdf).
- Lehtonen, M., O'Brien, H., 2009. Mantle transect of the Karelian Craton from margin to core based on P-T data from garnet and clinopyroxene xenocrysts in kimberlites. Bull. Geol. Soc. Finl. 81, 79–102. <https://doi.org/10.17741/bgsf/81.2.001>.
- Lehtonen, M., O'Brien, H., Peltonen, P., Johanson, B., Pakkanen, L., 2004. Layered mantle at the Karelian Craton margin: P–T of mantle xenocrysts and xenoliths from the Kaavi-Kuopio kimberlites, Finland. Lithos 77, 593–608. <https://doi.org/10.1016/j.lithos.2004.04.026>.
- Li, A., Burke, K., 2006. Upper mantle structure of southern Africa from Rayleigh wave tomography. J. Geophys. Res. 111, B10303. <https://doi.org/10.1029/2006JB004321>.
- Lubnina, N.V., Slabunov, A.I., 2011. Reconstruction of the Kenorland supercontinent in the Neoproterozoic based on Paleomagnetic and geological data. Mosc. Univ. Geol. Bull. 66 (4), 242–249. <https://doi.org/10.3103/S0145875211040077>.
- Miller, Yu.V., Milkevich, R.I., 1995. Cover-fold structure of the White Sea zone and its relationship with the Karelian granite-greenstone area. Geotektonika 6, 80–93 [In Russian]. (ISSN0016-853X).
- Mitrofanov, F.P., Sharov, N.V. (Eds.), 1998. Seismogeological model of the lithosphere of Northern Europe: Barents region. Apatity: KSC RAS 1998 (I), 237.
- Mitrofanov, F.P., Sharov, N.V., Zagorodny, V.G., Glaznev, V.N., Anna-Kaisi, Korja, 1998. Crustal Structure of the Baltic Shield along the Pechenga–Kostomuksha–Lovisa Geotraverse. Int. Geol. Rev. 40, 990–997. <https://doi.org/10.1080/00206819809465250>.
- NASEM (National Academies of Sciences, Engineering, and Medicine), 2020. A Vision for NSF Earth Sciences 2020–2030: Earth in Time. The National Academies, Washington, DC, p. 144. ISBNs: Paperback: 978-0-309-67600-7; Ebook: 978-0-309-67603-8. [10.17226/25761](https://doi.org/10.17226/25761).
- O'Brain, H.E., Peltonen, P., Vartiainen, H., 2005. Kimberlites, Carbonatites and alkaline rocks. In: Lehtinen, M., Nurm, P.A., Ramo, O.T. (Eds.), The Precambrian Geology of Finland – Key to the Evolution of the Fennoscandian Shield ISBN: 13: 9780444514219, Developments in Precambrian Geology, 14. Elsevier, Amsterdam, pp. 19–99.
- Peltonen, P., Brüggmann, G., 2006. Origin of layered continental mantle (Karelian craton, Finland): geochemical and Re-Os isotope constraints. Lithos 89, 405–423. <https://doi.org/10.1016/j.lithos.2005.12.013>.
- Peltonen, P., Kinnunen, K.A., Huhma, H., 2002. Petrology of two diamondiferous eclogite xenoliths from the Lahtojoki kimberlite pipe, eastern Finland. Lithos 63, 151–164. [https://doi.org/10.1016/S0024-4937\(02\)00119-6](https://doi.org/10.1016/S0024-4937(02)00119-6).
- Poli, P., Pedersen, H.A., Campillo, M., 2013. Noise directivity and group velocity tomography in a region with small velocity contrasts: the northern Baltic shield. Geophys. J. Int. 192, 413–424. <https://doi.org/10.1093/gji/ggs034>.
- Rosen, O.M., Manakov, A.V., Serenko, V.P., 2005. Paleoproterozoic collisional system and diamondiferous lithospheric keel of the Yakutian Kimberlite Province. Russ. Geol. Geophys. 46, 1237–1251. ISSN: 0016-7886.
- Rybakov, S.I., Svetova, A.I., Kulikov, V.S., Robonov, V.I., et al., 1981. Volcanism of the Archean Greenstone Belts of Karelia. Nedra, Leningrad, p. 154.
- Sandoval, S., Kissling, E., Ansorge, J., Korja, A., Seismic Tomography Work, S.V.E.K.A.L. A.P.K.O., Komminaho, K., 2004. High-resolution body wave tomography beneath the SVEKALAPKO array - II. Anomalous upper mantle structure beneath the Central Baltic Shield. Geophys. J. Int. 157 (1), 200–214. <https://doi.org/10.1111/j.1365-246X.2004.02131.x>.
- Seismic Handler, 2022. <https://www.seismic-handler.org/wiki>.
- Shaikh, A.M., Tappe, S., Bussweiler, Y., Patel, S.C., Ravi, S., Bolhar, R., Viljoen, F., 2020. Clinopyroxene and garnet mantle cargo in kimberlites as probes of Dharwar craton architecture and geotherms, with implications for post-1.1 Ga lithosphere thinning events beneath southern India. J. Petrol. 61, ega087. <https://doi.org/10.1093/ptrology/egaa087>.
- Sharov, N.V. (Ed.), 2001. Deep Structure and Evolution of the Earth's Crust in the Eastern Part of the Fennoscandian Shield: The Kem - Kalevala Profile. KarRC RAS, Petrozavodsk, p. 194.
- Sharov, N.V. (Ed.), 2004. Deep Structure and Seismicity of the Karelian Region and its Margins. KarRC RAS, Petrozavodsk, p. 365. <https://doi.org/10.3997/2214-4609.201402879>.
- Sharov, N.V., 2017. Lithosphere of Northern Europe: Seismic Data. KarRC RAS, Petrozavodsk, p. 173. ISBN: 978-5-9274-0741-5.
- Sharov, N.V., Slabunov, A.I., Isanina, Z.V., Krupnov, N.A., Roslov, Yu.V., Shchiptsova, N. I., 2010. Seismogeological section of the earth's fodder along the profile of the GSS-OGT "Susha-Sea" Kalevala - Kem - the throat of the White Sea. Geophys. J. 32, 21–34 (In Russian).
- Sharov, N.V., Bakunovich, L.I., Belashev, B.Z., Zhuravlev, V.A., Nilov, M.Yu., 2020. Geological-geophysical models of the crust for the White Sea region. Geodynam. Tectonophysics. 11, 566–582. <https://doi.org/10.5800/GT-2020-11-3-0491>.
- Silvennoinen, H., Kozlovskaya, E., Kissling, E., 2016. POLENET/LAPNET teleseismic P wave travel time tomography model of the upper mantle beneath northern Fennoscandia Solid. Earth 7, 425–439. <https://doi.org/10.5194/se-7-425-2016>.
- Slabunov, A.I., 2008. Geology and Geodynamics of the Archean Mobile Belts (On the Example of the White Sea (Belomorian) Province of the Fennoscandian Shield). KarRC RAS, Petrozavodsk, p. 298 [in Russian] ISBN: 978-5-9274-0349-3.
- Slabunov, A.I., Balagansky, V.V., Shchipansky, A.A., 2021. Mesoarchean to Paleoproterozoic crustal evolution of the Belomorian Province, Fennoscandian Shield, and the Tectonic Setting of Eclogites. Russ. Geol. Geophys. 62 (4), 525–546. <https://doi.org/10.15372/GiG2021116>.
- Slabunov, A.I., Lobach-Zhuchenko, S.B., Bibikova, E.V., Balagansky, V.V., Sorjonen-Ward, P., Volodichev, O.I., Shchipansky, A.A., Svetov, S.A., Chekulav, V.P., Arestova, N.A., Stepanov, V.S., 2006a. The Archean of the Baltic shield: geology, geochronology, and geodynamic settings. Geotectonics 40 (6), 409–433. <https://doi.org/10.1134/S001685210606001X>.
- Sokolov, V.A. (Ed.), 1987. Geology of Karelia. Leningrad, Nauka, p. 231.
- Sollogub, V.B. (Ed.), 1987. Lithosphere of Central and Eastern Europe: Geotraverse I, II, V. Nauk. Dumka, Kiev, p. 168.
- Tsvetkova, T.A., Shumlyanskaya, L.A., Bugaenko, I.V., Zaets, L.N., 2010. Seismotomography of the East European platform: a three-dimensional P-velocity model of the mantle near Fennoscandia. Part II. Geophys. J. 32, 60–77.
- Tsvetkova, T.A., Bugaenko, I.V., Zaets, L.N., 2019. Three-dimensional P-velocity model of the mantle and seismicity of Fennoscandia. Proc. KarRC RAS 2, 53–66. <https://doi.org/10.17076/geo861>.
- Vinnik, L.P., 1977. Detection of waves converted from P to SV in the mantle. Phys. Earth Planet. Inter. 15, 39–45. [https://doi.org/10.1016/0031-9201\(77\)90008-5](https://doi.org/10.1016/0031-9201(77)90008-5).
- Vinnik, L., Singh, A., Kiselev, S., Kumar, M.R., 2007. Upper mantle beneath foothills of the western Himalaya: subducted lithospheric slab or a keel of the Indian shield? Geophys. J. Int. 171, 1162–1171. <https://doi.org/10.1111/j.1365-246X.2007.03577.x>.
- Volodichev, O.I., 1990. Belomorian Complex of Karelia (Geology and Petrology). Nauka, Leningrad, p. 248.
- Windley, B.F., Kusky, T., Polat, A., 2021. Onset of plate tectonics by the Eoarchean. Precambrian Res. 35, 105980 <https://doi.org/10.1016/j.precamres.2020.105980>.
- Xu, Y.-G., 2001. Thermo-tectonic destruction of the Archean lithospheric keel beneath the Sino-Korean craton in China: evidence, timing and mechanism. Phys. Chem. Earth A 26, 747–757. [https://doi.org/10.1016/S1464-1895\(01\)00124-7](https://doi.org/10.1016/S1464-1895(01)00124-7).
- Zhuravlev, V.A., 2007. The crustal structure of the White Sea region. In: Razvedka i okhrana nedr \ Exploration and Conservation of Mineral Resources, 9, pp. 22–26 ([In Russian] ISSN 0034-026X).
- Zolotov, E.Ye., Kostyuchenko, S.L., Rakitov, V.A., et al., 2000. Inhomogeneities of the upper mantle of the Baltic shield according to seismic tomography data. Explor. Conserv. Min. Res. 2, 27–29 [In Russian]. (ISSN 0034-026X).
- Zozulya, D.R., Mitrofanov, F.P., Peltonen, P., O'Brien, H., Lehtonen, M., Kalachev, V.Yu., 2009. The structure of the lithospheric mantle and the prospects for diamond content in the Kola region (analysis of the chemistry and thermobarometry of kimberlite pyropes). Dokl. Earth Sci. 427 (5), 746–750. <https://doi.org/10.1134/S1028334X09050092>.